

Copper–Silica Nanocomposites Tailored by the Sol–Gel Route

Lidia Armelao,* Davide Barreca, and Gregorio Bottaro

ISTM-CNR and INSTM, Department of Chemistry, Padova University, Via Marzolo, 1-35131 Padova, Italy

Giovanni Mattei and Cinzia Sada

INFM and Department of Physics, Padova University, Via Marzolo, 8-35131 Padova, Italy

Eugenio Tondello

Department of Chemistry and INSTM, Padova University, Via Marzolo, 1-35131 Padova, Italy

Received October 7, 2004. Revised Manuscript Received December 14, 2004

Nanocomposite silica glassy layers (*host*) containing copper-based species (*guest*) were developed and tailored by the sol–gel route. The systems were obtained by starting from ethanolic solutions of tetraethoxysilane ($\text{Si}(\text{OC}_2\text{H}_5)_4$, TEOS) and copper(II) acetate ($\text{Cu}(\text{CH}_3\text{COO})_2 \cdot 4\text{H}_2\text{O}$) in a single-step process and subsequently annealed *ex situ* under different atmospheres (air, nitrogen, or 4% H_2 in N_2 mixture). In particular, the attention was focused on the possibility of tailoring the system composition and microstructure through a proper choice of the treatment temperatures (100–900 °C), duration (1–5 h), and environment. The composite evolution under annealing was investigated by glancing incidence X-ray diffraction, optical absorption spectroscopy, transmission electron microscopy, X-ray photoelectron spectroscopy, and atomic force microscopy. Pure copper–silica-based nanosystems, with guest composition ranging from CuO to Cu and controllable particle size and distribution, were obtained. The stepwise formation of CuO, Cu_2O , and Cu nanoclusters in the silica network as a function of the adopted conditions is critically discussed, highlighting the crucial points involved in the design and development of composites endowed with peculiar chemicophysical properties.

Introduction

A great scientific and technological interest is increasingly being devoted to insulator glasses doped with metal or semiconductor nanocrystals, for the development of novel devices with enhanced functional properties.¹ In this context, copper-silica based systems are endowed with interesting characteristics which make them suitable for many applications. Silica glasses (*host*) containing copper oxides (*guest*) are attractive candidates for catalysis, solid-state lasers, sensors, and colored coatings.^{2,3} Various chemical and physical methods have been used for the preparation of embedded copper oxide nanoparticles, and depending on the adopted synthetic route, CuO, Cu_2O , or both phases with different crystallite size have been obtained.^{4–10}

On the other hand, metallic Cu nanoclusters homogeneously dispersed in silica layers have attracted great attention for the development of nonlinear optical devices.^{11–14} Consequently, in the synthesis of copper–silica host–guest systems, beyond the control on crystallite size and distribution, a major concern is represented by the tailoring of the copper oxidation state in the guest particles. This goal can be pursued by a proper combination of preparation procedures and processing conditions, paying particular attention to the redox processes involving copper-containing species during thermal treatments.

The sequential pathway occurring at molecular or atomic level for the change in copper oxidation state from II in CuO to 0 in metallic Cu is still a current subject of investigation. In particular, the involved mechanisms are strongly dependent on the nature of the copper source as well as on the system microstructure, morphology, and texture, resulting in different evolutions for powders, aerogels, xerogels, and

* Corresponding author. Phone: +39-0498275236. Fax: +39-0498275161. E-mail: armelao@chin.unipd.it.

- (1) El-Sayed, M. A. *Acc. Chem. Res.* **2001**, *34*, 257.
- (2) Dutta, A.; Das, D.; Grilli, M. L.; Di Bartolomeo, E.; Traversa, E.; Chakravorty, D. J. *Sol–Gel Sci. Technol.* **2003**, *26*, 1085.
- (3) Paulose, P. I.; Jose, G.; Thomas, V.; Jose, G.; Unnikrishnan, N. V.; Warrior, M. K. R. *Bull. Mater. Sci.* **2002**, *25*, 69.
- (4) Battaglin, G.; Cattaruzza, E.; Gonella, F.; Polloni, R.; Scremin, B. F.; Mattei, G.; Mazzoldi, P.; Sada, C. *Appl. Surf. Sci.* **2004**, *226*, 52.
- (5) Borgohain, K.; Singh, J. B.; Rama Rao, M. V.; Shripathi, T.; Mahamuni, S. *Phys. Rev. B* **2000**, *61*, 11093.
- (6) Brookshier, M. A.; Chusuei, C. C.; Goodman, D. W. *Langmuir* **1999**, *15*, 2043.
- (7) Balamurugan, B.; Mehta, B. R.; Shivaprasad, S. M. *Appl. Phys. Lett.* **2001**, *79*, 3176.
- (8) Palkar, V. R.; Pushan, A.; Chattopadhyay, S.; Multani, M. *Phys. Rev. B* **1996**, *53*, 2167.
- (9) Basu, S.; Das, D.; Chakravorty, D. J. *Appl. Phys.* **2004**, *95*, 5741.

- (10) Mohanan, J. L.; Brock, S. L. *Chem. Mater.* **2003**, *15*, 2567.
- (11) Pérez-Robles, J. F.; García-Rodríguez, F. J.; Yáñez-Limón, J. M.; Espinoza-Beltrán, F. J.; Vorobiev, Y. V.; González-Hernández, J. J. *Phys. Chem. Solids* **1999**, *60*, 1729.
- (12) Cattaruzza, E.; Battaglin, G.; Calvelli, P.; Gonella, F.; Mattei, G.; Maurizio, C.; Mazzoldi, P.; Padovani, S.; Polloni, R.; Sada, C.; Scremin, B. F.; D'Acapito, F. *Compos. Sci. Technol.* **2003**, *63*, 1203.
- (13) Manikandan, D.; Mohan, S.; Nair, K. G. M. *Mater. Lett.* **2004**, *58*, 907.
- (14) Uchida, K.; Kaneko, S.; Omi, S.; Hata, C.; Tanji, H.; Asahara, Y.; Ikushima, A. J.; Tokizaki, T.; Nakamura, A. J. *Opt. Soc. Am. B* **1994**, *11*, 1236.

thin films, depending on the preparation route.^{15–18} As a consequence, a detailed comparison between results obtained in different conditions becomes extremely complicated.

Among the synthesis routes, the sol–gel process is a versatile low-temperature approach to glass coatings and powdered samples incorporating nanoclusters in various matrixes.^{19–22} Moreover, under suitable conditions, the formation of the host and guest phases in the composite system can be performed by a *single-step* process. This peculiarity, together with the mild synthesis conditions (*soft chemistry*), makes the sol–gel method particularly suitable for yielding thin films with good control over composition and microstructure. To our knowledge, there are only a few available reports on the formation of copper-based nanosystems by sol–gel to date.^{2,3,10,11,20,22–30}

In this study we report the results for the sol–gel synthesis of CuO, Cu₂O, and Cu nanocrystals in silica glassy layers. The *as-prepared* samples contain only Cu(II) cations which evolve to *tenorite* (CuO), *cuprite* (Cu₂O), or metallic Cu crystallites after thermal treatments in different conditions (annealing temperature, duration, and atmosphere). In this way, the guest phase composition as well as the growth and size distribution of the clusters in the silica matrix have been controlled and tailored. However, a remarkable difference with respect to other studies concerns the role played by the annealing procedure on the investigated samples. In the present study, the samples are subjected to thermal treatments immediately after preparation. In these conditions, annealing promotes simultaneously nucleation, growth, and redox processes. Consequently, the behavior and evolution of a nondensified Cu(II)–SiO_x(OH)_y macromolecular network is expected to be deeply different with respect to that of systems containing preformed crystalline CuO particles. In this regard, preliminary results concerning the system evolution in air have already been shortly reported.³¹

Experimental Section

Synthesis. Composite silica coatings containing copper and copper oxide nanoclusters were prepared from ethanolic solutions of tetraethoxysilane [Si(OCH₂CH₃)₄, TEOS, Aldrich, 99.9%] and copper(II) acetate [Cu(CH₃COO)₂·4H₂O, Aldrich, 98%].

In the preparation of copper–silica nanosystems, the best results were achieved by mixing an ethanolic (CH₃CH₂OH, Carlo Erba, 99.8%) solution of copper acetate to prehydrolyzed TEOS (TEOS: HCl:H₂O:CH₃CH₂OH = 1:28:0.5:20) aged under continuous stirring at room temperature for 60 h. The adopted Cu/TEOS molar ratios were 0.1 and 0.2. Higher copper concentrations were not taken into account in order to prevent aggregation/coalescence phenomena during the system evolution. Furthermore, it is worth highlighting that most of the advanced applications require the use of *diluted* nanocomposites with small and well-dispersed clusters in the host medium.¹⁴

The obtained clear, green-colored sols were aged for 1 h at room temperature before use.

Film deposition was carried out at room temperature in air, by dip-coating on Herasil silica slides (Heraeus, Quarzschmelze, Hanau, Germany). Coatings were obtained by means of a multi-dipping process, up to three depositions, without any thermal treatment between them and a controlled withdrawal speed of 7 cm × min^{−1}. The as-prepared samples, were subsequently heated at temperatures between 100 and 900 °C. The treatment time was varied between 1 and 5 h in three different flowing atmospheres, i.e., oxidizing (air), inert (nitrogen; purity, 5.0) and reducing (mixture of 4% H₂ in N₂; purity, 5.0).

Characterization. Glancing incidence X-ray diffraction (GIXRD) measurements were performed by a D8 ADVANCE Bruker diffractometer equipped with a Cu Kα source (40 kV, 40 mA) and a Göbel mirror, at a fixed incidence angle of 1.5°. The crystallite dimensions were estimated from the most intense peaks by means of the Scherrer equation.

Optical absorption spectra of the films were recorded in the range 400–800 nm on a Cary 5E (Varian) UV–vis–near-IR dual-beam spectrophotometer with a spectral bandwidth of 2 nm. In each spectrum, the silica substrate contribution was subtracted.

Transmission electron microscopy (TEM) analyses were performed both in conventional and high-resolution (HRTEM) modes with a FEI TECNAI F20 SuperTwin (S)TEM field-emission (FEG) microscope operating at 200 kV equipped with an EDAX energy-dispersive X-ray spectrometer (EDS) for compositional micro-analysis.

X-ray photoelectron spectra were recorded by a Perkin-Elmer Φ 5600ci spectrometer using monochromatized Al Kα radiation (1486.6 eV). Depth profiles were carried out by Ar⁺ sputtering at 2.5 keV with an argon partial pressure of 5 × 10^{−6} Pa. Charge neutralization with a low-energy electron flood gun was adopted. The residual shift on the reported binding energy (BE) values was corrected by assigning to the C1s line of adventitious carbon a value of 284.8 eV.

Atomic force micrographs were recorded by a NT-MDT SPM Solver P47H-PRO instrument operating in tapping mode and in air. Images were recorded in different sample areas in order to check surface homogeneity.

Results and Discussion

Microstructure. The nanocomposite systems were first analyzed by GIXRD. With regard to the more diluted

- (15) Epifani, M.; De, G.; Licciulli, A.; Vasanelli, L. *J. Mater. Chem.* **2001**, *11*, 3326.
- (16) De Sousa, E. M. B.; De Sousa, A. P. G.; Mohallem, N. D. S.; Lago, R. M. *J. Sol–Gel Sci. Technol.* **2003**, *26*, 873.
- (17) Rodríguez, J. A.; Kim, J. Y.; Hanson, J. C.; Pérez, M.; Frenkel, A. I. *Catal. Lett.* **2003**, *85*, 247.
- (18) Kim, J. Y.; Rodríguez, J. A.; Hanson, J. C.; Frenkel, A. I.; Lee, P. L. *J. Am. Chem. Soc.* **2003**, *125*, 10684.
- (19) Armelao, L.; Bertoncello, R.; DeDominicis, M. *Adv. Mater.* **1997**, *9*, 736.
- (20) Das, D.; Chakravorty, D. *Appl. Phys. Lett.* **2000**, *76*, 1273.
- (21) Brinker, C. J.; Scherer, G. W. *Sol–Gel Science: The Physics and Chemistry of Sol–Gel Processing*; Academic Press: New York, 1990.
- (22) Gurin, V. S.; Alexeenko, A. A.; Yumashev, K. V.; Prokoshin, R.; Zolotovskaya, S. A.; Zhavnerko, G. A. *Mater. Sci. Eng., C* **2003**, *23*, 1063.
- (23) Manzanares-Martínez, J.; García-Cerda, L. A.; Ramírez-Bon, R.; Espinoza-Beltrán, F. J.; Pérez-Robles, J. F.; González-Hernández, J. *Thin Solid Films* **2000**, *365*, 30.
- (24) Lutz, T.; Estourès, C.; Merle, J. C.; Guille, J. L. *J. Alloys Compd.* **1997**, *262*, 438.
- (25) Nogami, M.; Abe, Y.; Nakamura, A. *J. Mater. Res.* **1995**, *10*, 2648.
- (26) Pérez-Robles, F.; García-Rodríguez, F. J.; Jiménez-Sandoval, S.; González-Hernández, J. *J. Raman Spectrosc.* **1999**, *30*, 1099.
- (27) Maruse, N.; Kuraoka, K.; Yazawa, T. *Mol. Cryst. Liq. Cryst.* **1998**, *314*, 273.
- (28) de Sousa, E. M. B.; Guimaraes, A. P.; Mohallem, N. D. S.; Lago, R. M. *Appl. Surf. Sci.* **2001**, *183*, 216.
- (29) Mendoza-Galván, A.; Pérez-Robles, J. F.; Espinoza-Beltrán, F. J.; Ramirez-Bon, R.; Vorobiev, Y. V.; González-Hernández, J.; Martinez, G. *J. Vac. Sci. Technol., A* **1999**, *17*, 1103.

- (30) Cordoba, G.; Arroyo, R.; Fierro, J. L. G.; Viniegra, M. *J. Solid State Chem.* **1996**, *123*, 93.
- (31) Armelao, L.; Barreca, D.; Bertapelle, M.; Bottaro, G.; Sada, C.; Tondello, E.; *Mater. Res. Soc. Symp. Proc.* **2003**, *737*, F8.27.1

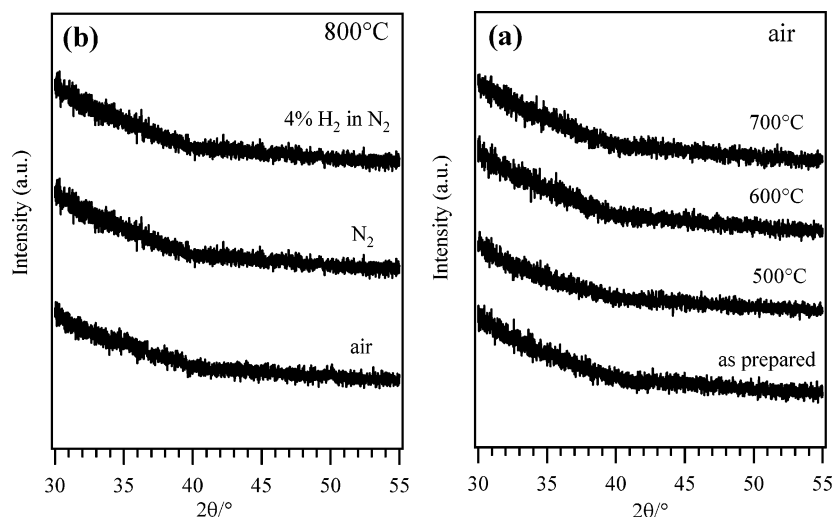


Figure 1. GIXRD patterns for the more diluted samples ($\text{Cu}:\text{Si} = 0.1$ in the starting sols) corresponding to different annealing temperatures and atmospheres. In all cases the annealing time was 1 h.

composites ($\text{Cu}:\text{Si} = 0.1$ in the starting sol), no diffraction peaks were ever observed irrespective of the annealing conditions, as exemplified in Figure 1.

The absence of crystalline phases might be attributed either to the very small cluster sizes or to the low amount of crystalline phases, due to both the high dilution of copper-containing species in the silica matrix and the use of thin films. On the basis of these results, the attention was focused on the analysis of copper–silica-based nanosystems obtained from more concentrated sols ($\text{Cu}:\text{Si} = 0.2$), to attain a deeper insight into their microstructural evolution by a joint GIXRD and TEM characterization. For these specimens, annealing in air (Figure 2a) did not result in any detectable diffraction peak up to 600 °C. At 700 °C, a weak reflection ($2\theta = 35.5^\circ$) ascribed to CuO (tenorite) crystallization [(002), (−111)] was observed. Prolonged treatments, up to 5 h, at higher temperatures (900 °C), promoted the system crystallization (Figure 2a), as indicated by the intensity increase of the [(002), (−111)] peak and the rising of the (111) ($2\theta = 38.7^\circ$) and (−202) ($2\theta = 48.7^\circ$) signals of cupric oxide. The mean CuO crystallite size was 14 nm. Because of the absence of ternary phases in the CuO– SiO_2 composition diagram, copper oxide particles could be formed from phase segregation by annealing silica samples containing dispersed copper species.¹⁰

The formation and stability of crystalline clusters containing reduced copper species were studied by treating the as-prepared samples in N_2 and in H_2 (4% in N_2) fluxes. Similarly to the results obtained in air, tenorite was the first observed crystalline phase (Figure 2b) when the crude copper–silica layers were treated under inert atmosphere at 700 °C (1 h), whereas an evolution in the system composition was observed at higher temperatures. In the diffraction pattern of the sample annealed at 900 °C for 3 h, besides the tenorite reflections, two weak diffraction lines attributed to the Cu_2O (cuprite) ($2\theta = 36.4^\circ$ (111) and 42.3° (200)) were detected, along with a peak at $2\theta = 43.3^\circ$ corresponding to (111) planes of metallic copper.

A prolonged treatment at 900 °C (up to 5 h) induced the growth of Cu_2O diffraction peaks as well as the disappear-

ance of Cu reflections. The mean diameter of cuprite nanocrystallites was lower than 24 nm, irrespective of the treatment conditions. The formation of cuprite after annealing in nitrogen is ascribed to the low stability of CuO in oxygen-deficient atmospheres.^{17,32} This behavior is expected considering that bulk CuO decomposes to Cu_2O at ≈ 1000 °C.

Concerning the systems annealed in reducing atmosphere, no diffraction peaks were observed for annealing up to 600 °C, whereas tenorite crystallites were detected at higher temperatures (Figure 2c). The effect of the H_2 – N_2 mixture on the system composition and microstructure was well-evidenced after heating at 900 °C for 1 h. In the corresponding GIXRD spectrum (Figure 2c), tenorite peaks were accompanied by the (111) reflection of metallic copper at $2\theta = 43.3^\circ$. Annealing at 900 °C (up to 5 h) resulted in the progressive increase of the Cu (111) peak and the rising of the (200) ($2\theta = 50.4^\circ$) one at the expense of the CuO crystal phase, even if tenorite was still present in the sample. For the complete $\text{Cu(II)} \rightarrow \text{Cu(0)}$ conversion, the use of higher temperatures was discarded, since they approach the thermodynamic melting points of copper oxides ($T_m(\text{CuO}) = 1336$ °C ($P(\text{O}_2) = 1$ atm), $T_m(\text{Cu}_2\text{O}) = 1230$ °C). Taking into account the size-dependent properties of nanoclusters, more severe conditions were not adopted to avoid undesired processes and reactions between the guest species and the silica matrix. As an alternative route, previously N_2 -treated $\text{Cu}_2\text{O}:\text{SiO}_2$ specimens were subjected to annealing in H_2 – N_2 atmosphere under the most severe tested conditions (Figure 2d). The resulting GIXRD spectrum clearly displayed two intense reflections ((111) and (200)) associated to metallic copper (average crystallite size, ca. 20 nm), whereas no appreciable contribution from CuO and/or Cu_2O phases could be observed. The different behavior between tenorite and cuprite could be tentatively explained by considering that the reduction reaction might require different induction times in the two cases.^{17,18,33}

(32) Ragone, D. V. *Thermodynamics of Materials*; Wiley: New York, 1995.

(33) Kung, H. H. *Transition Metal Oxides: Surface Chemistry and Catalysis*; Elsevier: New York, 1995.

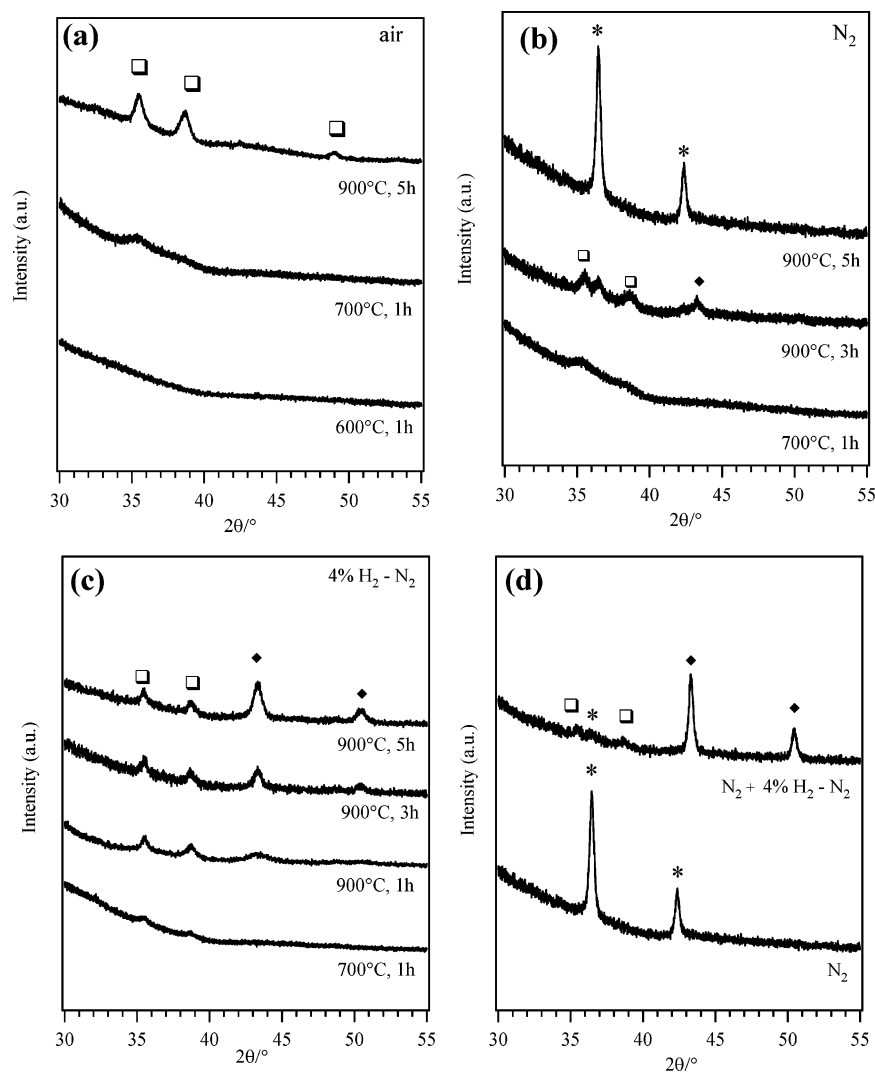


Figure 2. GIXRD spectra for samples annealed under different conditions in (a) air, (b) N₂, (c) 4% H₂–N₂ mixture, and (d) for a specimen annealed at 900 °C for 5 h in N₂ and subsequently treated at 900 °C for 5 h in 4% H₂–N₂ mixture. The markers in the figure indicate the CuO (□), Cu₂O (*), and Cu (◆) crystal phases.

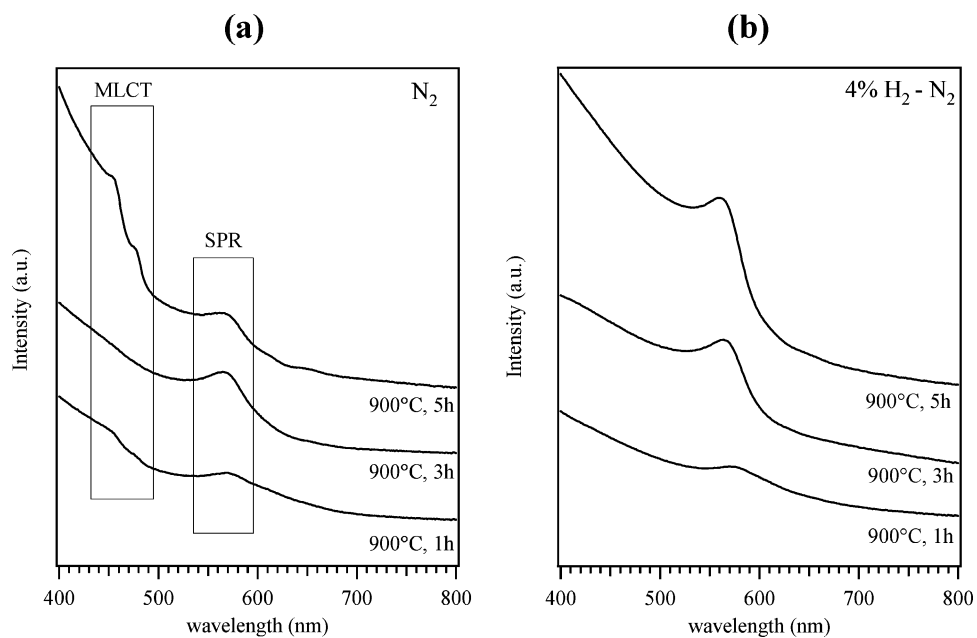


Figure 3. Optical absorption spectra of copper–silica nanocomposites annealed under different conditions in (a) N₂ and (b) 4% H₂–N₂ mixture.

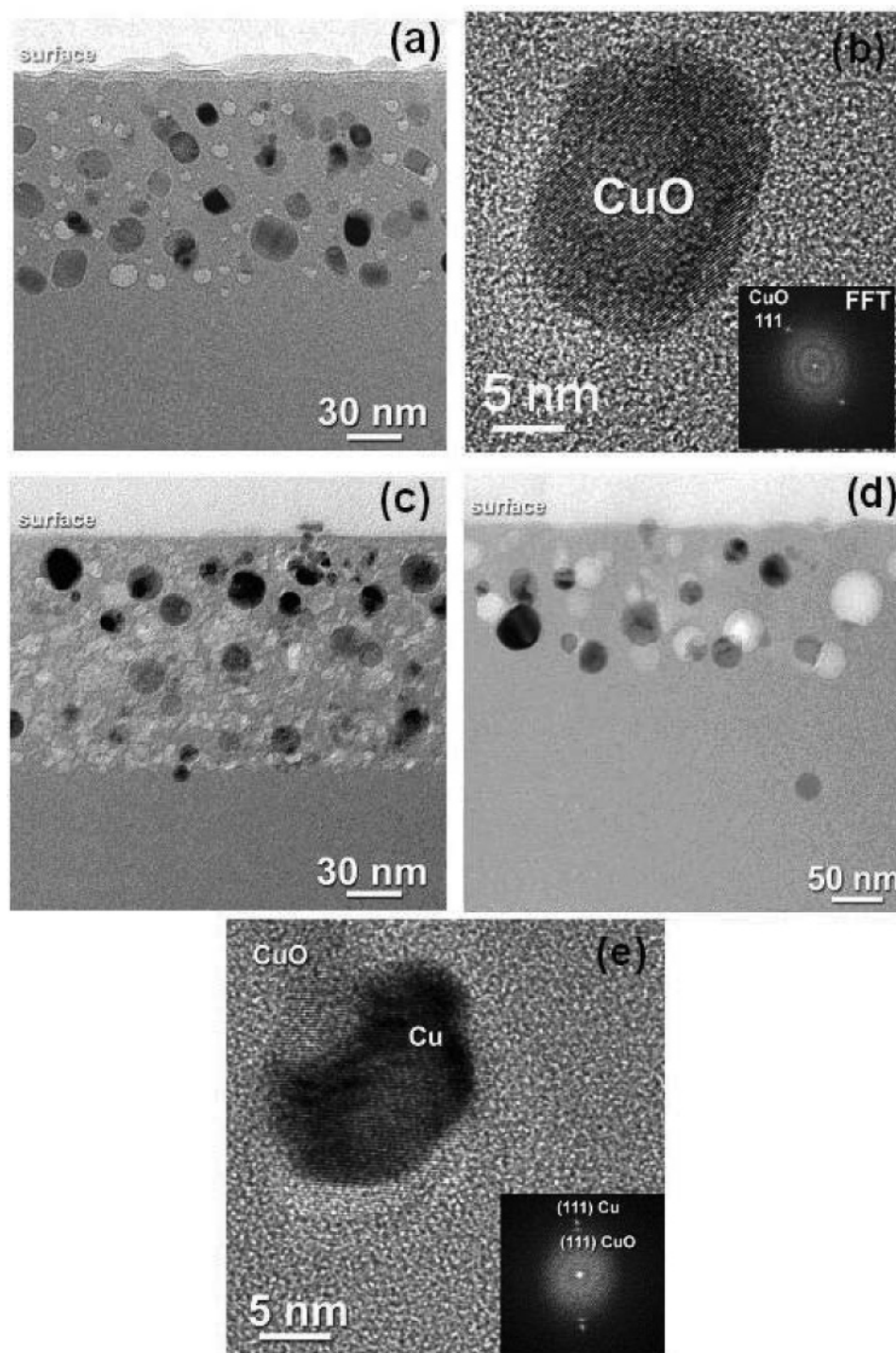


Figure 4. Representative TEM cross-sectional micrographs for a copper-silica nanocomposite annealed at 900 °C, 5 h in air (a and b), N₂ (c), N₂ and subsequently in H₂-N₂ mixture (d and e).

Representative optical absorption spectra for samples subjected to annealing in nitrogen at 900 °C for different times are reported in Figure 3a.

In agreement with the red sample color, a common feature of all spectra was the presence of an absorption peak centered at 560 nm, the characteristic surface plasmon resonance (SPR) band of metallic Cu nanoclusters in a silica matrix.^{4,34} Moreover, Cu₂O presence was further ascertained by two absorptions centered at 450 and 480 nm, attributed to metal-ligand charge transfers (MLCTs).^{24,35}

The reduction of Cu(II) centers, resulting in the formation of copper nanoclusters, was well-evidenced by UV-vis

spectra. In fact, samples treated in H₂-N₂ atmosphere at 900 °C for 1 h (Figure 3b) clearly displayed the SPR peak of metallic copper nanoclusters.

The optical spectra evolution was in good agreement with GIXRD results. Prolonged annealing at 900 °C favored a progressive Cu(II) → Cu(0) reduction, as confirmed by the intensity increase of both the SPR band (Figure 3b) and the (111) and (200) diffraction peaks of metallic copper (Figure

(34) Kreibitz, U.; Vollmer, M. *Optical Properties of Metal Clusters*; Springer-Verlag: Berlin, 1995.

(35) Arujo, R. J.; Butty, J.; Peyghambarian, N. *Appl. Phys. Lett.* **1996**, 68, 29.

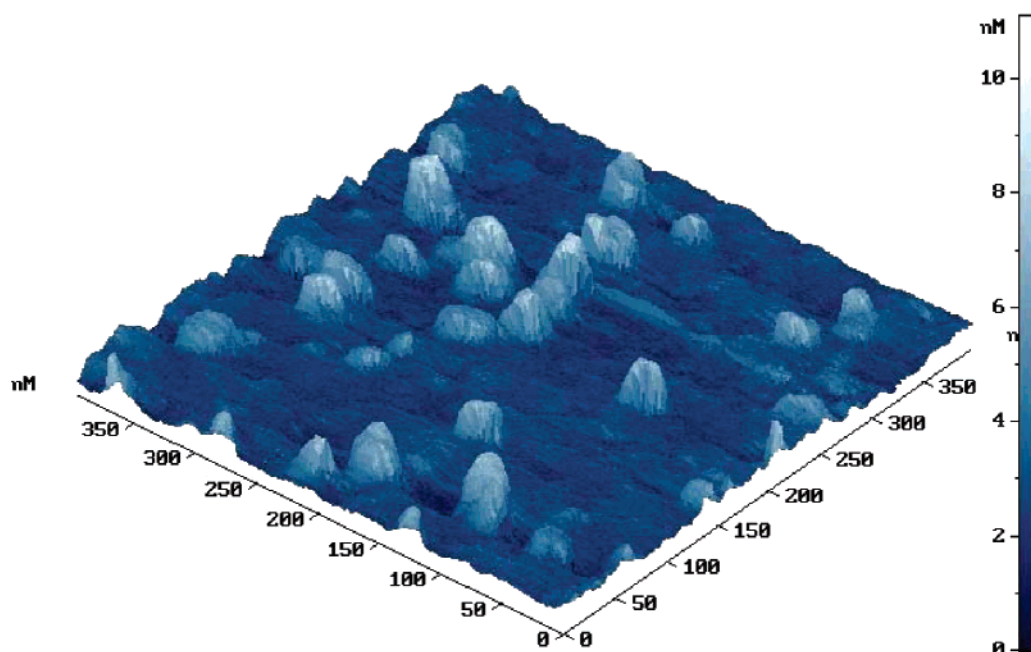


Figure 5. AFM image for a copper–silica nanocomposite annealed at 900 °C, 5 h in a mixture of 4% H_2 – N_2 .

2c). The present data suggest that a complete conversion to Cu(0) would require more severe reducing conditions. Indeed, TEM measurements (see below) suggested that both Cu_2O and metallic copper were present in the SiO_2 matrix.

To attain a deeper insight on the cluster distribution in the host matrix, selected samples were subjected to TEM analyses.

Figure 4a displays a bright field cross-sectional micrograph of a specimen annealed in air at 900 °C for 5 h. The composition deduced by HRTEM (Figure 4b) and energy dispersion spectroscopy (EDS) analysis on single clusters corresponded to CuO , in agreement with GIXRD results. CuO nanoaggregates were homogeneously distributed in a silica layer 130 nm thick. This observation unambiguously confirmed the formation of a $\text{CuO}:\text{SiO}_2$ nanocomposite system. As a general trend, the nanocrystals did not exhibit a spherical shape, showing instead some faceting. To obtain a size distribution, an average evaluation over major and minor axes was performed. The corresponding particle size distribution was fitted by a Gaussian function yielding an average diameter $\langle D \rangle = 12$ nm and a standard deviation $\sigma = 5$ nm, in accordance with the crystallite size estimated by GIXRD analysis. In fact, the HRTEM images of CuO nanoclusters (Figure 4b) evidenced that they were single-crystalline rather than multiparticle agglomerates. It is worth highlighting the presence of a residual porosity in the analyzed specimen, despite the severe treatment conditions, even though EDS compositional analysis confirmed the nominal stoichiometry of the silica matrix. Nevertheless, N_2 BET adsorption analyses on the investigated specimens were not attempted due to the very low material amount, preventing any further information on the system porosity.

Concerning nitrogen-annealed samples (900 °C, 5 h), a homogeneous distribution of spherical clusters (with a $\langle D \rangle = 14$ nm and $\sigma = 5$ nm) in silica was observed (Figure 4c). Selected area electron diffraction (SAED) and EDS analyses indicated that, in agreement with GIXRD data, most of the

clusters were made of Cu_2O and only a small fraction was constituted by pure Cu, as can be also deduced from the SPR peak in the optical spectra (Figure 3b). The sol–gel silica matrix retained a porous structure even after annealing up to 900 °C. Prolonged treatments at the same temperature resulted in a complete film densification, as displayed in Figure 4d (corresponding to an additional annealing in H_2 – N_2 atmosphere for 5 h), where the sol–gel silica could not be distinguished from the SiO_2 substrate.

In the case of the sample annealed at 900 °C first in N_2 for 5 h and subsequently in the H_2 – N_2 mixture for 5 h, some clusters exhibited a partial core–shell structure, in which a Cu core was partially surrounded by a CuO shell. This structure is shown in the HRTEM image of Figure 4e, whose Fourier transform indicated the presence in the nanocluster of (111) planes of both metallic Cu and CuO .

Morphology. The formation of copper-containing clusters was further ascertained by AFM imaging. As an example, Figure 5 displays the surface morphology of a specimen annealed at 900 °C, 5 h in reducing atmosphere.

The micrograph was dominated by the presence of uniformly distributed globular nanoaggregates with average dimensions of ≈ 22 nm and root-mean-square roughness of 1.3 nm. The surface presence of copper-containing agglomerates opens intriguing perspectives for an eventual use of the obtained nanocomposites in gas-sensing devices.

Chemical Composition. Surface and in-depth chemical composition was analyzed by XPS. Irrespective of the processing conditions, all specimens presented Cu, O, Si, and C signals. The latter arose only from atmospheric contamination, as proved by its disappearance after a mild Ar^+ sputtering. All the analyzed composites revealed the presence of Cu(II) species on the surface, as indicated by the Cu $2p_{3/2}$ position (BE = 933.7 eV) and the presence of appreciable intense *shake-up* satellites, typical of Cu(II) oxidation state.^{36–38} This result could be interpreted by taking into account that the outermost specimen layers were always

oxidized to CuO-related species due to contact with outer atmosphere.

Concerning the spatial distribution of copper nanoclusters in the sol-gel silica matrix, in-depth XPS analyses agreed to a good extent with cross-sectional TEM observations. As a matter of fact, copper-containing species resulted homogeneously distributed in the silica matrix throughout the system thickness. Moreover, it is worth evidencing that the experimental Cu:Si ratio was very close to the nominal one in the starting precursor solution.

Conclusions

Copper-silica nanocomposites, with copper in the form of both metal and/or Cu₂O/CuO, were obtained by a single-step sol-gel route starting from copper(II) acetate and TEOS as precursors for guest and host, respectively. Irrespective of the annealing conditions, a homogeneous distribution of copper-containing clusters in the sol-gel silica matrix was observed. Tenorite was stable in air in a wide temperature range. Conversely, treatment under inert atmosphere resulted

in the formation of nanometric Cu₂O aggregates only after heating at 900 °C for 5 h. Finally, Cu:SiO₂ nanocomposites were obtained after annealing under reducing atmospheres. The CuO phase resulted stable even in these conditions, as proved by its presence even after 5 h treatment at 900 °C in H₂-N₂ atmosphere. Moreover, HRTEM analysis evidenced the partial core-shell correlation between Cu and CuO phases in nitrogen and H₂-N₂ annealed samples. Finally, the presence of metallic copper nanoparticles even in Cu₂O:SiO₂ samples obtained by annealing in nitrogen was evidenced. Prolonged treatment resulted in a complete silica densification, making the host matrix undistinguishable from the substrate.

As a whole, the results presented in this work point to the possibility of obtaining silica-copper nanocomposites in the form of thin films and with well-tailored compositional and microstructural features by an adequate choice of processing conditions.

Acknowledgment. Italian Research Programs FIRB-MIUR "Nano-organization of hybrid inorganic/organic molecules with magnetic and optical properties", FISR-MIUR "Molecular nanotechnologies for information storage and transmission", and FIRB-MIUR-RBNE019H9K "Molecular manipulation for nanomachinery" provided financial support for this work.

CM048245O

-
- (36) Armelao, L.; Barreca, D.; Bertapelle, M.; Bottaro, G.; Sada, C.; Tondello, E. *Thin Solid Films* **2003**, *442*, 48.
(37) Briggs, D.; Seah, M. P. *Practical Surface Analysis*; Wiley: Chichester, U.K., 1990; Vol. 1.
(38) McIntyre, N. S.; Cook, M. G. *Anal. Chem.* **1975**, *47*, 2208.